



Article

# Neuroprotective and Anti-Inflammatory Effects of Kuwanon C from *Cudrania tricuspidata* Are Mediated by Heme Oxygenase-1 in HT22 Hippocampal Cells, RAW264.7 Macrophage, and BV2 Microglia

Wonmin Ko <sup>1,†</sup>, Chi-Su Yoon <sup>2,3,†</sup>, Kwan-Woo Kim <sup>2,3</sup>, Hwan Lee <sup>1</sup>, Nayeon Kim <sup>1</sup>, Eun-Rhan Woo <sup>1</sup>, Youn-Chul Kim <sup>2</sup>, Dae Gill Kang <sup>3</sup>, Ho Sub Lee <sup>3</sup>, Hyuncheol Oh <sup>2,3</sup> and Dong-Sung Lee <sup>1,\*</sup> 

<sup>1</sup> College of Pharmacy, Chosun University, Dong-gu, Gwangju 61452, Korea; rabis815@naver.com (W.K.); ghksldi123@hanmail.net (H.L.); rlaskdus1209@naver.com (N.K.); wooer@Chosun.ac.kr (E.-R.W.)

<sup>2</sup> Institute of Pharmaceutical Research and Development, College of Pharmacy, Wonkwang University, Iksan 54538, Korea; ycs1991@naver.com (C.-S.Y.); swamp1@naver.com (K.-W.K.); yckim@wku.ac.kr (Y.-C.K.); hoh@wonkwang.ac.kr (H.O.)

<sup>3</sup> Hanbang Cardio-Renal Syndrome Research Center, Wonkwang University, Iksan 54538, Korea; dgkang@wku.ac.kr (D.G.K.); host@wku.ac.kr (H.S.L.)

\* Correspondence: dslee2771@chosun.ac.kr; Tel.: +82-62-230-6386; Fax: +82-62-222-5414

† These authors contributed equally to this work.

Received: 19 June 2020; Accepted: 6 July 2020; Published: 8 July 2020



**Abstract:** Heme oxygenase (HO)-1 is a detoxifying phase II enzyme that plays a role in both inflammatory and oxidative stress responses. *Cudrania tricuspidata* is widespread throughout East Asia and is used as a therapeutic agent in traditional medicine. We investigated whether treatment with sixteen flavonoid or xanthone compounds from *C. tricuspidata* could induce HO-1 expression in HT22 hippocampal cells, RAW264.7 macrophage, and BV2 microglia. In these compounds, kuwanon C showed the most remarkable HO-1 expression effects. In addition, treatment with kuwanon C reduced cytoplasmic nuclear erythroid 2-related factor (Nrf2) expression and increased Nrf2 expression in the nucleus. Significant inhibition of glutamate-induced oxidative injury and induction of reactive oxygen species (ROS) occurred when HT22 hippocampal cells were pretreated with kuwanon C. The levels of inflammatory mediator and cytokine, which increased following lipopolysaccharide (LPS) stimulation, were suppressed in RAW264.7 macrophage and BV2 microglia after kuwanon C pretreatment. Kuwanon C also attenuated p65 DNA binding and translocation into the nucleus in LPS-induced RAW264.7 and BV2 cells. The anti-inflammatory, anti-neuroinflammatory, and neuroprotective effects of kuwanon C were reversed when co-treatment with HO-1 inhibitor of tin protoporphyrin-IX (SnPP). These results suggest that the neuroprotective and anti-inflammatory effects of kuwanon C are regulated by HO-1 expression.

**Keywords:** heme oxygenase-1 regulation; *Cudrania tricuspidata*; kuwanon C; HT22 hippocampal cells; BV2 microglia; RAW264.7 macrophage

## 1. Introduction

Heme oxygenase (HO) catalyzes the degradation of heme and is found in three isoforms: HO-1, -2, and -3. HO-1 is a 32 kDa protein induced by diverse stimuli, including inflammatory cytokine expression and oxidative stress. HO-2 is a 36 kDa protein that commonly acts as an important constitutively expressed enzyme, and HO-3 is a 33 kDa protein important for heme sensing [1,2].

HO-1 is a detoxifying phase II enzyme that plays a critical role in both inflammatory and oxidative responses. HO-1-mediated degradation of heme generates carbon monoxide (CO), biliverdin, and iron, which are believed to facilitate several cytoprotective responses against oxidative stress [3]. Nuclear erythroid 2-related factor (Nrf2) regulates the expression of various cytoprotective genes, including HO-1. In addition, Nrf2 is known to serve an essential function in both the xenobiotic and oxidative stress responses, fulfilling a critical protective function in several organs, including the kidney, liver, nervous system, and lungs [4].

Neurodegenerative diseases such as Parkinson's, Huntington's, and Alzheimer's disease, are characterized by dysfunction of the central nervous system (CNS) and progressive loss of neurons. Neuroinflammation and chronic oxidative stress are considered the main causes of these diseases, implying that HO-1 plays a key role in preventing pathogenesis through the regulation of inflammatory and oxidative stress responses [5].

*Curdrania tricuspidata* (Moraceae family) is widespread throughout East Asia and is a common ingredient in many traditional medicines. *C. tricuspidata* contains several classes of potentially therapeutic compounds, including xanthenes, flavonoids, organic acids, and phenylpropanoids. Several studies have attempted to classify the abundant xanthenes and flavonoids produced by these plants. In addition, *C. tricuspidata* is known to produce pharmacological activity, including anti-inflammatory, antioxidant, antitumor, hepatoprotective, neuroprotective, anti-obesity, antimicrobial, immunomodulatory, antiatherosclerotic, skin-protecting, and anti-diabetic effects [6]. In our previous study, we evaluated several *C. tricuspidata* compounds and their effects on HO-1 expression and reported that two compounds exert their biological effects through the regulation of HO-1 expression. Other studies have reported that cudratricusxanthone A exerts a protective effect on HT22 cells and has an anti-inflammatory effect in RAW264.7 cells [7,8]. In addition, cudraflavanones A have been shown to exert anti-neuroinflammatory effects in BV2 cells [9].

This study identifies new bioactive compounds from *C. tricuspidata* and describes their activity in various cell lines. In total, sixteen compounds were evaluated in neurodegenerative and inflammatory disease models. This study focused on identifying biomarkers that regulate the expression of HO-1 in three cell lines of neurodegenerative and inflammatory disease model: the immortalized murine hippocampal neuronal cell line HT22, the murine-derived macrophage cell line RAW264.7, and the immortalized murine microglia cell line BV2.

## 2. Results

### 2.1. Effects of Sixteen Compounds from *C. tricuspidata* on the Viability of HT22, RAW264.7, and BV2 Cells

The sixteen *C. tricuspidata* compounds used in this study were all isolated from the roots of the plant using our previously described isolation method. In addition, the chemical structures for these compounds, dihydrokaempferol (1), steppogenin (2), cudraflavanone A (3), cudraxanthone L (4), cudraflavone C (5), cudraflavanone D (6), kuwanon C (7), cudratricusxanthone A (8), macluraxanthone B (9), cudraxanthone M (10), 1,6,7-trihydroxy-2-(1,1-dimethyl-2-propenyl)-3-methoxyxanthone (11), cudraxanthone D (12), cudratricusxanthone N (13), cudraflavanone B (14), cudratricusxanthone L (15), and cudratricusxanthone A (16), have also been previously described [10]. To determine the cytotoxic effects of these compounds (CTC; *C. tricuspidata* compound, Figure 1), we treated HT22, RAW264.7, and BV2 cells with various concentrations of each compound for 24 h and subsequently performed an 3-(4,5-dimethylthiazol-2-yl)-2,5-diphenyltetrazolium bromide (MTT) assay (Supplementary Figures S1–S3). These MTT assays were then used to determine the highest nontoxic dosage of each compound, which was subsequently used in all experiments.

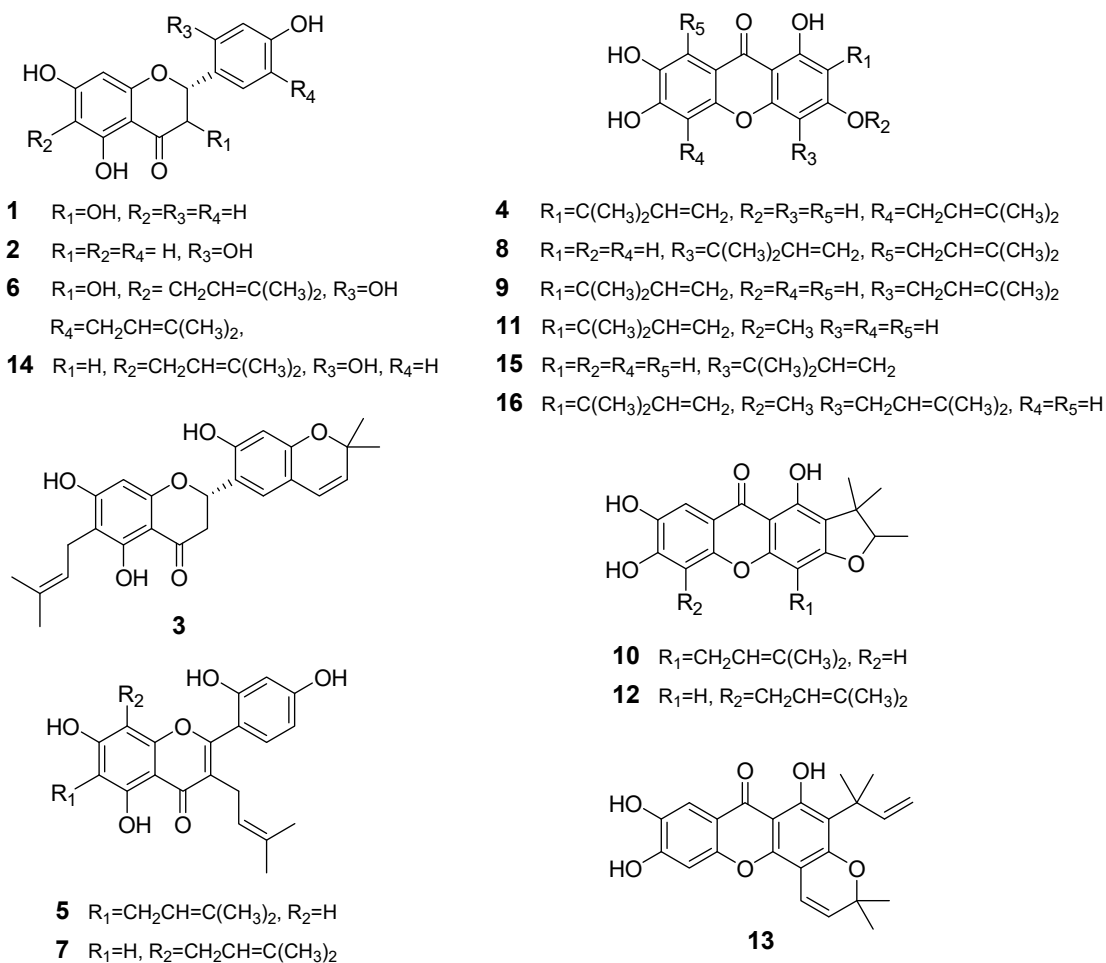


**Figure 1.** Chemical structures of the sixteen *C. tricuspidata* compounds used in this study.

## 2.2. Effects of the Sixteen *C. tricuspidata* Compounds on HO-1 Protein Expression and Nuclear Translocation of Nrf2 in HT22, RAW264.7, and BV2 Cells

To investigate whether any of these compounds induced the expression of HO-1 in HT22, RAW264.7, and BV2 cells were treated with the indicated concentrations of each of the test compounds for 12 h and then assayed by Western blotting. Cobalt protoporphyrin (CoPP), an established HO-1 inducer, was used as a positive control. CTC **2, 3, 4, 7, 9, 10,** and **12** significantly induced HO-1 expression in HT22 cells (Figure 2), whereas **3, 7, 9, 14,** and **15** induced HO-1 expression in RAW264.7 cells (Figure 3) and CTC **1, 2, 3, 7, 9, 10, 11, 12, 13, 14,** and **15**.

HO-1 expression in BV2 cells (Figure 4). CTC **3** and **7** were able to induce significant HO-1 expression in all three cell lines, with CTC **7** exhibiting the strongest induction. Thus, we examined the effect of CTC **7** treatment on the nuclear translocation of activated Nrf2. For this purpose, HT22, RAW264.7, and BV2 cells were treated with 40  $\mu$ M CTC **7** for 0.5, 1, and 1.5 h, and Nrf2 expression was assayed using Western blotting. This assay showed that CTC **7** treatment induced the nuclear translocation of Nrf2 in a time-dependent manner (Figure 5).

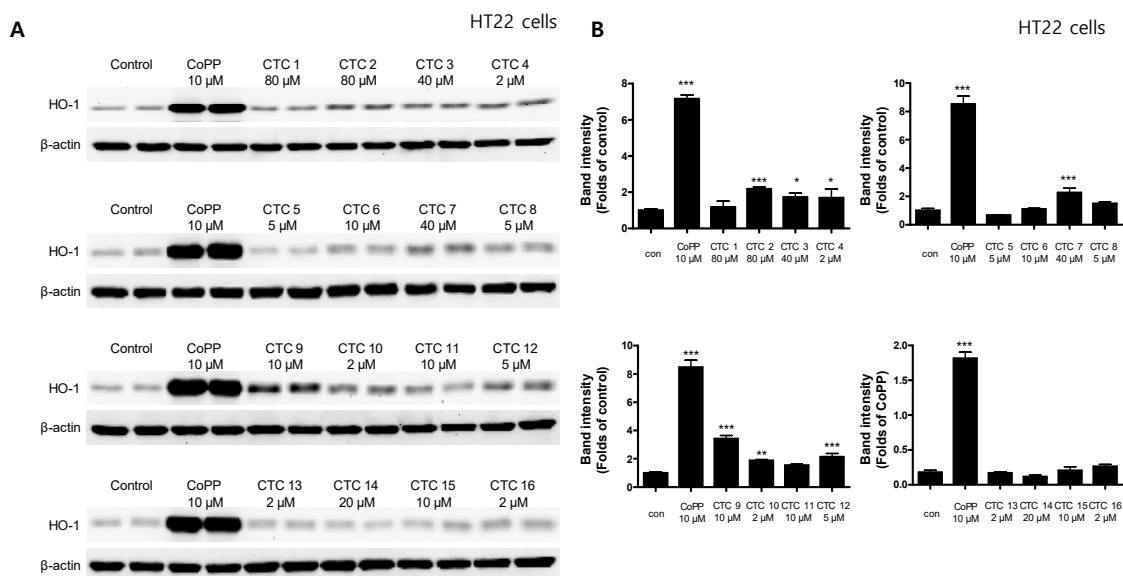


**Figure 2.** Effects of each of the sixteen *C. tricuspidata* compounds on the protein expression levels of HO-1 in HT22 cells. (A) Cells were treated for 12 h with the indicated concentration of each compound and assayed using Western blotting. Immunoblotting was performed using ImageJ software. (B) Band intensities were normalized to  $\beta$ -actin. CoPP (10  $\mu$ M) was used as a positive control. Data are presented as the mean  $\pm$  standard deviation of four independent experiments. \*  $p < 0.05$ , \*\*  $p < 0.01$ , \*\*\*  $p < 0.001$  when compared to the untreated control.

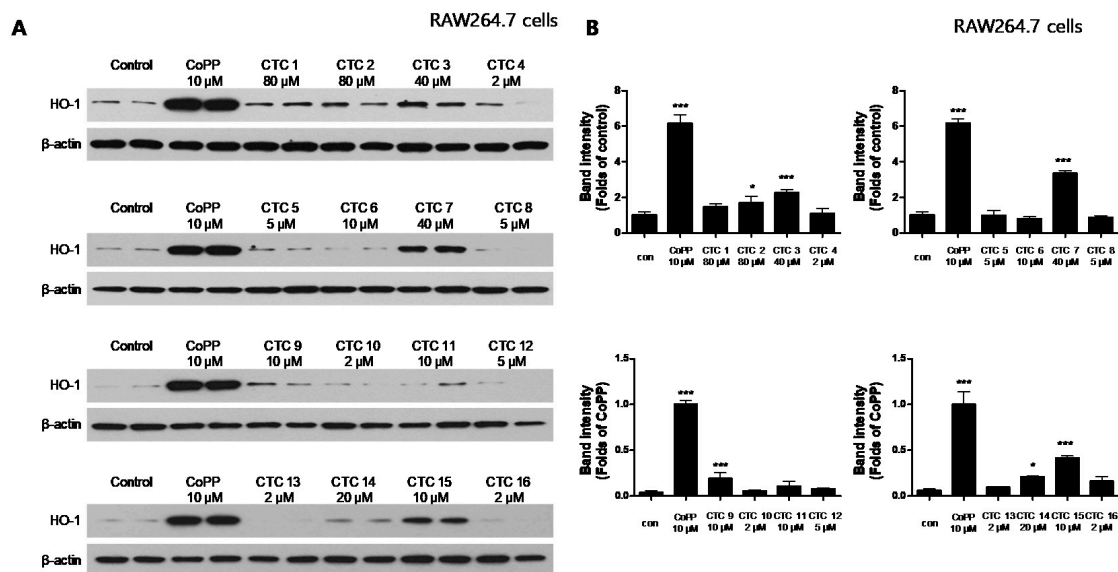


**Figure 3.** Effects of the sixteen *C. tricuspidata* compounds on the protein expression levels of HO-1 in RAW264.7 cells. (A) Cells were incubated for 12 h with the indicated concentration of each compound and analyzed using western blotting. (B) Band intensities were normalized to  $\beta$ -actin. CoPP (10  $\mu$ M) was used as a positive control. Data are presented as the mean  $\pm$  standard deviation of four independent experiments. \*  $p < 0.05$ , \*\*\*  $p < 0.001$  when compared to the control group.

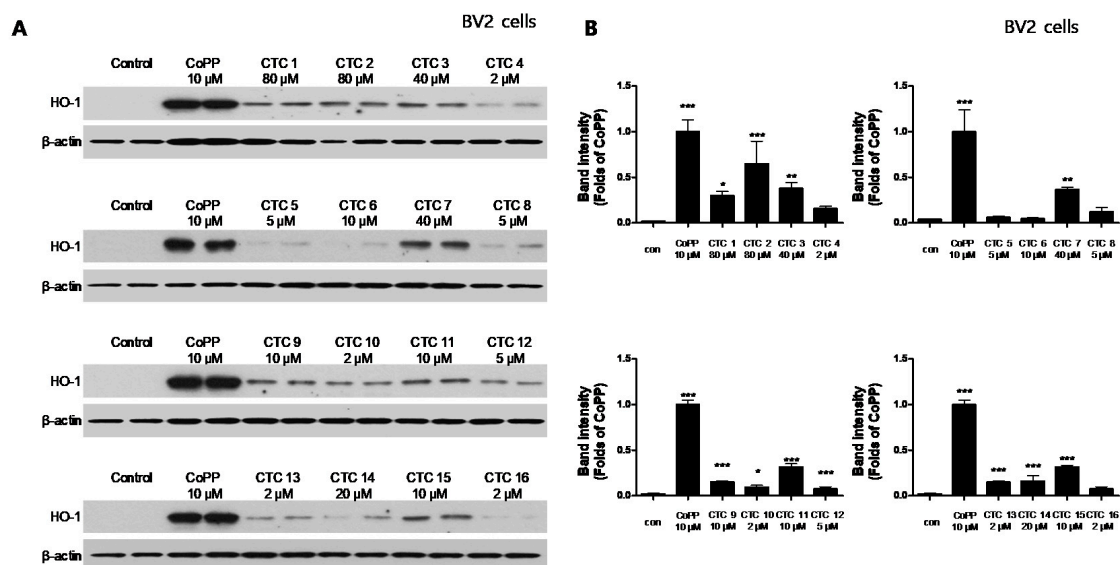


**Figure 4.** Effects of the sixteen *C. tricuspidata* compounds on the protein expression levels of HO-1 in BV2 cells. (A) Cells were incubated for 12 h with the indicated concentration of each compound and analyzed using western blotting. (B) Band intensities were normalized to  $\beta$ -actin. CoPP (10  $\mu$ M) was used as a positive control. Data are presented as the mean  $\pm$  standard deviation of four independent experiments. \*  $p < 0.05$ , \*\*  $p < 0.01$ , \*\*\*  $p < 0.001$  when compared to the control group.

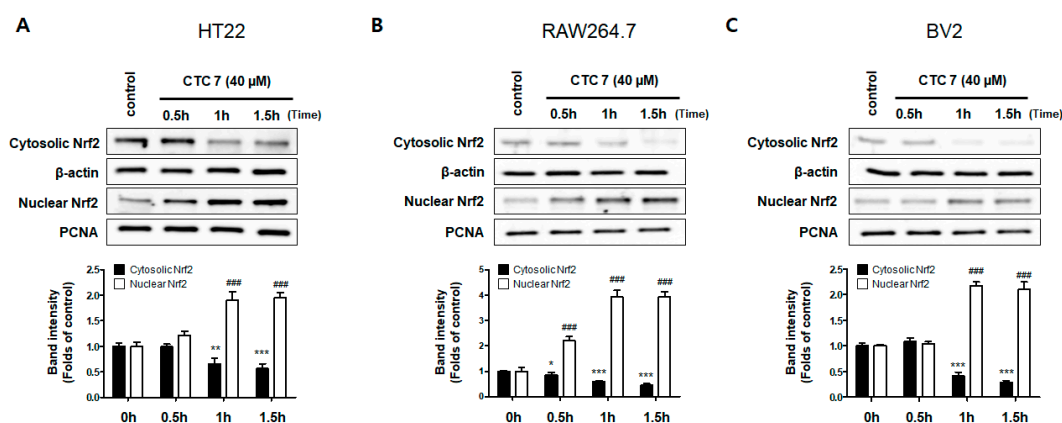


**Figure 5.** Effects of CTC 7 treatment on the nuclear translocation of nuclear factor erythroid-derived 2-related factor-2 (Nrf2) in HT22 (A), RAW264.7 (B), and BV2 (C) cells. These cells were treated with CTC 7 (40  $\mu$ M) for 0.5, 1, or 1.5 h and then the nuclei were fractionated from the cytosol using a Caiman Nuclear Extraction Kit. Cytoplasmic and nuclear Nrf2 expression was then assayed using western blotting. Data represent the mean  $\pm$  standard deviation for three independent experiments. \*  $p < 0.05$ , \*\*  $p < 0.01$ , \*\*\*  $p < 0.001$  when compared to the untreated cytosolic Nrf2 control. ###  $p < 0.001$  when compared to the untreated nuclear Nrf2 control.

### 2.3. Effect of CTC 7 Treatment on Glutamate-Induced Oxidative Injury and Reactive Oxygen Species (ROS) Generation in HT22 Cells

Based on the observation that CTC 7 treatment induced HO-1 protein expression in HT22, RAW264.7, and BV2 cells, we examined the neuroprotective capacity of CTC7 treatment, its anti-oxidative stress and anti-inflammatory effects, following lipopolysaccharide (LPS) challenge in HT22 cells. HT22 cells were pretreated with CTC 7 for 3 h and exposed to glutamate (10 mM) for 12 h. Pretreatment of HT22 cells with 20 or 40  $\mu$ M of CTC 7 significantly reduced the effects of glutamate-induced oxidative injury (Figure 6A). In addition, pretreatment with 20 or 40  $\mu$ M CTC 7 for 3 h also effectively decreased ROS production induced by glutamate treatment (Figure 6B).

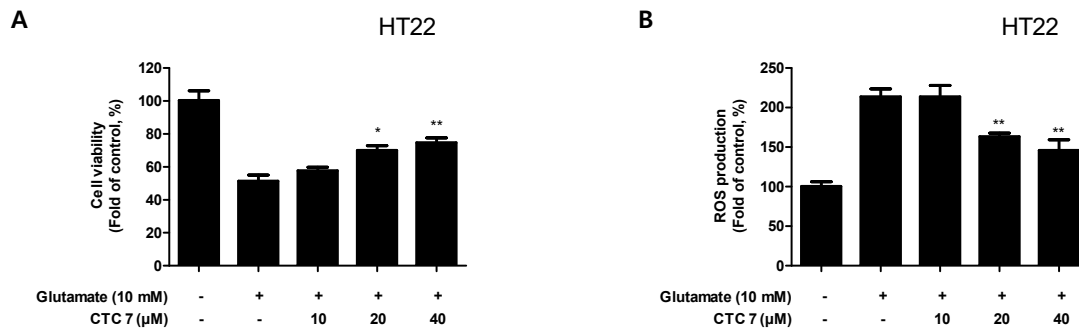


**Figure 6.** Effects of CTC 7 treatment on glutamate-induced (A) oxidative neurotoxicity and (B) ROS generation in HT22 cells. HT22 cells were pretreated with CTC 7 (10, 20, and 40  $\mu$ M) for 3 h and then incubated with glutamate (10 mM) for 12 h. Data are presented as the mean  $\pm$  standard deviation for three independent experiments. \*  $p < 0.05$ , \*\*  $p < 0.01$  when compared to glutamate-treated cells.

#### 2.4. Effects of CTC 7 Treatment on LPS-Induced Production of Nitric Oxide (NO), Prostaglandin E<sub>2</sub> (PGE<sub>2</sub>), Interleukin (IL)-6, and Tumor Necrosis Factor (TNF)- $\alpha$ , and the Expression of Inducible Nitric Oxide Synthase (iNOS) and Cyclooxygenase (COX)-2 in RAW264.7 and BV2 Cells

Given these results, we determined whether CTC 7 treatment could attenuate the overproduction of the proinflammatory mediators NO, PGE<sub>2</sub>, IL-6, and TNF- $\alpha$  in RAW264.7 and BV2 cells stimulated with LPS (1  $\mu$ g/mL). The levels of NO, PGE<sub>2</sub>, IL-6, and TNF- $\alpha$  increased following LPS stimulation, and pretreatment with CTC 7 suppressed these responses in both RAW264.7 and BV2 cells (Figure 7). Furthermore, the expression of iNOS and COX-2 proteins increased in LPS-treated groups, and these responses were also repressed in cells pretreated with CTC 7 (Figure 8).

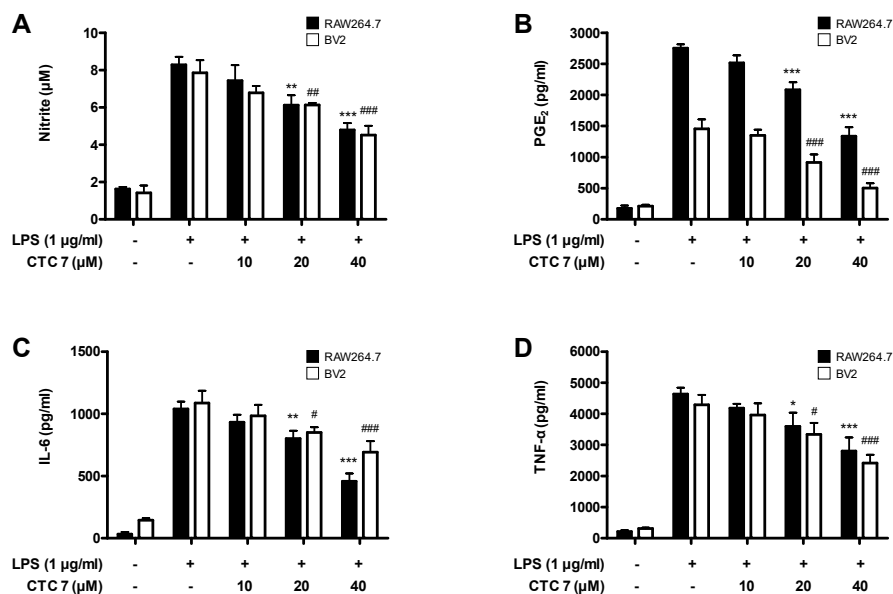


**Figure 7.** Effects of CTC 7 treatment on nitrite content (A) PGE<sub>2</sub> (B), IL-6 (C), and TNF- $\alpha$  (D) expression in LPS-stimulated RAW264.7 and BV2 cells. Cells were pretreated for 3 h with the indicated concentrations of CTC 7 and stimulated for 24 h with LPS (1  $\mu$ g/mL). Measurements of nitrite concentrations, a PGE<sub>2</sub> assay, and an enzyme-linked immunosorbent assay (ELISA) were performed as described in the Materials and Methods. Bars represent the mean  $\pm$  standard deviation for three independent experiments. \*  $p < 0.05$ , \*\*  $p < 0.01$ , \*\*\*  $p < 0.001$ , #  $p < 0.05$ , ##  $p < 0.01$ , ###  $p < 0.001$  compared with the LPS-treated group.

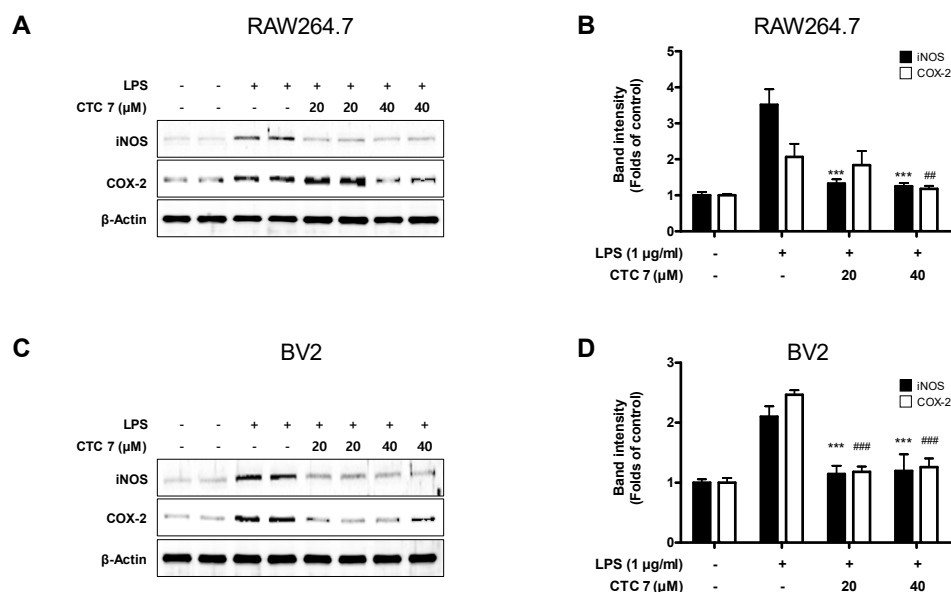


**Figure 8.** Effects of CTC 7 treatment on the protein expression levels of iNOS (A) and COX-2 (B) in LPS-stimulated RAW264.7 and BV2 cells. Cells were pretreated for 3 h with the indicated concentrations of CTC 7 and stimulated for 24 h with LPS (1 µg/mL). Western blot analysis was performed as described in the Materials and Methods. Immunoblotting was performed using ImageJ software. Band intensities were normalized to that of β-actin. \*\*\*  $p < 0.001$ , ##  $p < 0.01$ , ###  $p < 0.001$  when compared with the LPS-treated control.

### 2.5. Effect of CTC 7 Treatment on LPS-Induced Activation of Nuclear Factor Kappa B (NF-κB) Signaling in RAW264.7 and BV2 Cells

Activation of the NF-κB signaling pathway is required for LPS-induced production of proinflammatory mediators [11]. Therefore, we investigated whether CTC 7 treatment affects the activation of the NF-κB signaling pathway in LPS-induced RAW264.7 and BV2 cells. Cells were pretreated with CTC 7 for 3 h and stimulated with LPS for 1 h. The DNA binding activity of p65 was shown to increase the response to LPS stimulation, and pretreatment with CTC 7 attenuated this DNA binding activity in both RAW264.7 and BV2 cells (Figure 9A). In addition, immunofluorescence analysis showed that the p65 subunit was translocated into the nucleus following LPS stimulation and that pretreatment with CTC 7 blocked this response in both RAW264.7 (Figure 9B) and BV2 cells (Figure 9C).

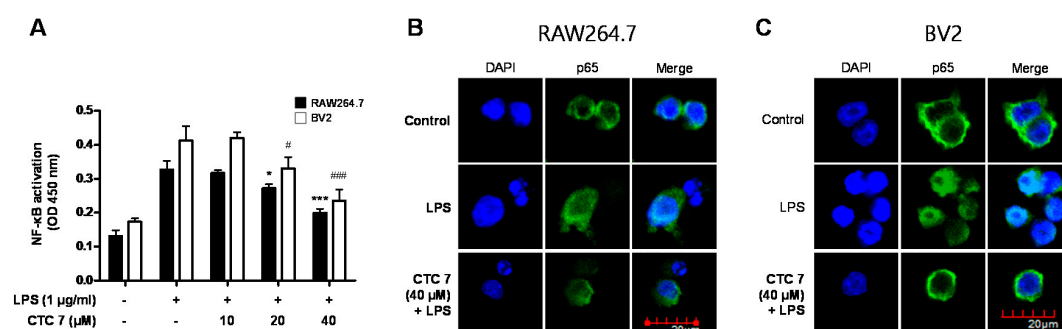


**Figure 9.** Effects of CTC 7 treatment on NF-κB DNA-binding activity (A) and NF-κB localization (B,C) in RAW264.7 and BV2 cells. Cells were pretreated with the indicated concentrations of CTC 7 for 3 h and stimulated with LPS (1 µg/mL) for 1 h. A commercially available NF-κB ELISA kit was used to test nuclear extracts and determine the level of NF-κB binding in each of the samples. Data represent the mean values of three independent experiments. \*  $p < 0.05$ , \*\*\*  $p < 0.001$ , #  $p < 0.05$ , ###  $p < 0.001$  when compared to the LPS-treated control.

### 2.6. Effect of CTC 7 Treatment on LPS-Induced NF- $\kappa$ B Activation in RAW264.7 and BV2 Cells

To determine whether the neuroprotective and anti-inflammatory effects of CTC 7 are correlated with HO-1 expression in HT22, RAW264.7, and BV2 cells, we included a set of experiments with tin protoporphyrin-IX (SnPP), which is a selective HO-1 inhibitor. After the cells were treated with 40  $\mu$ M CTC 7 for 3 h with or without 50  $\mu$ M SnPP, the cells were treated with glutamate for another 12 h (HT22) or LPS for 24 h (RAW264.7 and BV2 cells) and assayed by ELISA. Pretreatment with CTC 7 protected HT22 cells against glutamate-induced oxidative injury (Figure 10A) by reducing ROS production in these cells (Figure 10B). However, these responses were effectively eliminated by the simultaneous addition of SnPP (Figure 10A,B). SnPP did not affect cell viability or ROS production in glutamate-treated HT22 cells, suggesting that these changes were the result of the direct inhibitory effect of SnPP on HO-1. In addition, pretreatment with CTC 7 resulted in decreased nitrite and TNF- $\alpha$  production in LPS-induced RAW264.7 (Figure 10C,D) and BV2 (Figure 10E,F). However, the anti-inflammatory effects of CTC 7 were also reversed by SnPP in both cell types. Similar to HT22 cells, SnPP alone did not affect NO or TNF- $\alpha$  production following LPS stimulation, which suggests that the neuroprotective and anti-inflammatory effects of CTC 7 treatment are regulated by HO-1 expression.

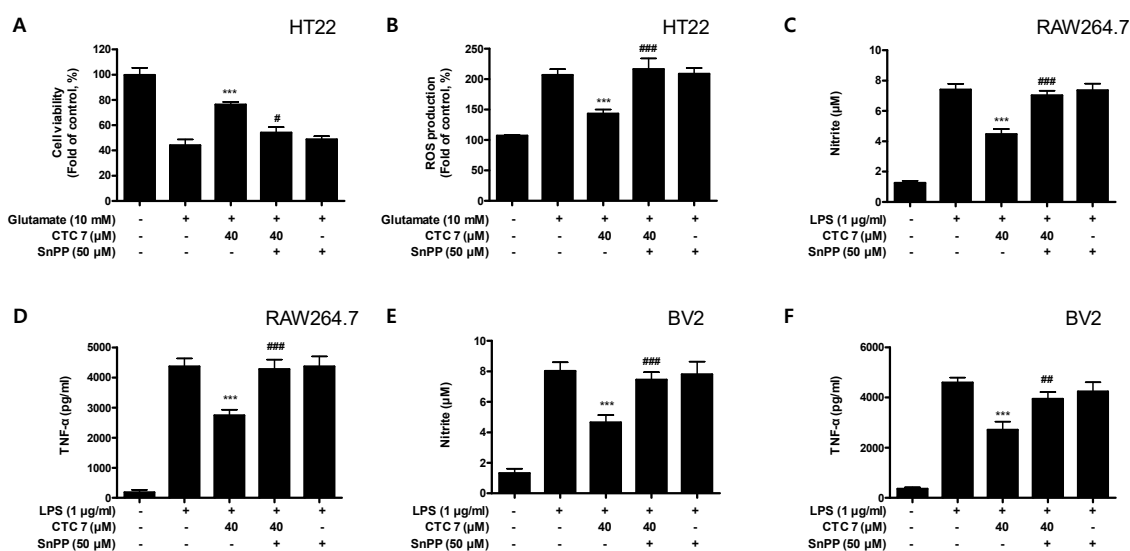


**Figure 10.** Effects of CTC 7-induced Nrf2-mediated HO-1 expression on glutamate-induced oxidative neurotoxicity and ROS generation in HT22 (A,B) cells and LPS-stimulated proinflammatory mediator production in RAW264.7 (C,D) and BV2 (E,F) cells. HT22 cells were treated with CTC 7 (40  $\mu$ M) in the presence or absence of SnPP (50  $\mu$ M). (A) Cell viability and (B) ROS generation were measured following treatment with glutamate (10 mM) for 12 h. RAW264.7 and BV2 cells were pretreated with CTC 7 (40  $\mu$ M) for 3 h with or without SnPP (50  $\mu$ M), and subsequently stimulated with LPS (1  $\mu$ g/mL) for 24 h. Nitrite (C,E) and TNF- $\alpha$  (D,F) were assayed as described in the Materials and Methods section. Data are presented as the mean  $\pm$  standard deviation for three independent experiments. \*\*\*  $p < 0.001$  compared to the glutamate or LPS control; #  $p < 0.05$ , ##  $p < 0.01$ , ###  $p < 0.001$  compared to CTC7 plus glutamate or LPS without SnPP.

### 3. Discussion

HO-1 enzymes have been used as important markers in the regulation of various diseases, including obesity and vascular diseases [12], kidney injury [13], diabetes [14], and digestive disorders [15]. HO-1 expression has also been linked to neuroprotective and neurotoxic effects, and it is upregulated in brain tissues following various oxidative stress-inducing pathological stimuli [5,16]. In addition, it has been reported that CO production through heme degradation by HO-1 exerts anti-inflammatory effects [17]. Many studies have shown that various types of natural products regulate HO-1 expression, which we confirmed in a recent study, suggesting that one of the pathways for its



regulation could be the Nrf-2 pathway [18–20]. Accordingly, this study focused on the discovery and validation of natural products that exert a regulatory effect on inflammatory and degenerative diseases via changes in HO-1 expression. First, we confirmed the cytotoxic effects of the sixteen compounds (Supplementary Figures S1–S3) and evaluated their effects on HO-1 expression in HT22, BV2, and RAW264.7 cells. A total of seven compounds (Steppogenin, cudraflavanone A, cudraxanthone L, kuwanon C, macluraxanthone B, cudraxanthone M, and cudraxanthone D) in HT22 (Figure 2), five compounds (steppogenin, cudraflavanone A, kuwanon C, macluraxanthone B, and 16,7-trichydroxy-2-(1,1-dimethyl-2-propenyl)-3-methyloxanthone) in RAW264.7 cells (Figure 3), and nine compounds (dihydrokaempferol, steppogenin, cudraflavanone A, kuwanon C, macluraxanthone B, cudraxanthone M, 1,6,7-trihydroxy-2-(1,1-dimethyl-2-propenyl)-3-methoxyxanthone, cudraxanthone D, and cudraflavanone B) in BV2 cells (Figure 4) were shown to significantly upregulate HO-1 expression. Of these, four compounds—steppogenin, cudraflavanone A, kuwanon C, and macluraxanthone B—were shown to affect HO-1 expression in all three cell lines including HT22, BV2, and RAW264.7.

Steppogenin of flavanone skeletons has been studied for its cyclooxygenase [21] and tyrosinase inhibitory effects [22–26]. In our previous study, we showed that steppogenin altered the anti-neuroinflammatory response via NF- $\kappa$ B and mitogen-activated protein kinase (MAPK) signaling suppression in microglia [27]. Cudraflavanone A, a prenylated flavanone, has been reported to inhibit topoisomerase I and protein kinase C (PKC) activity, leading to the induction of apoptotic cell death in human cancer cells [28] and vascular smooth muscle cell growth via a protein kinase B (Akt)-dependent pathway [29]. Our previous study also reported the anti-neuroinflammatory effects of cudraflavanone A via induction of HO-1 expression [9]. Macluraxanthone B, a prenylated xanthone, has been shown to exert anti-human immunodeficiency virus (HIV) [30], hepatoprotective [31], cytotoxic [32], and antitumor effects [33]. Kuwanon C, a prenylated flavone, has been shown to exert a number of biological effects, including an inhibitory effect on platelet aggregation induced by platelet-activating factor (PAF) and arachidonic acid [34], mild cyclooxygenase inhibition, strong lipoxysgene inhibition [35], tyrosinase inhibition [36,37], anti-microbial effects [38], melanin inhibition [39], cytotoxic effects [40,41], cholinesterase inhibition [42], skin whitening effects [43], anti-obesity effects [44], anti-inflammatory effects on only reducing of NO production [44–46], antioxidant effects [47], mild cathepsin K inhibition [48], pancreatic lipase inhibition [49], protective effects in a spinal cord injury model [50], antiproliferative effects [51], and attenuation of MPTP-induced Parkinson's disease [52]. As a result of this study, among the sixteen compounds, kuwanon C showed the most remarkable effect for inducing HO-1 in all of three cells, and this is first report to biological action of kuwanon C though the HO-1 regulation in the HT22 hippocampal, BV2 microglia, and RAW264.7 macrophage cells. Therefore, we conducted further study of kuwanon C in three cell lines.

The Nrf2 transcription factor plays an important role in antioxidant responsive element (ARE)-mediated expression of phase 2 detoxifying genes and in the activation of other inducible genes, including HO-1 [53]. A previous study showed that the induction of HO-1 is primarily regulated at the transcriptional level, and its induction is often related to Nrf2 activation. Therefore, regulating the degree of oxidative stress via upregulation of Nrf2-mediated HO-1 may be an important factor in developing a treatment strategy for neurological diseases [54]. As a result, we confirmed that kuwanon C treatment induces the translocation of Nrf2 to the nucleus in HT22, BV2, and RAW264.7 cell lines (Figure 5). Neuronal oxidative stress has been postulated to be the underlying basis for neuronal cell death in neurodegenerative diseases [55,56], and HT22 hippocampal cells have played a critical role in developing neurodegenerative disease models. Glutamate is known to generate oxidative stress, leading to the depletion of glutathione, elevated  $\text{Ca}^{2+}$  levels, and increased ROS production [57]; however, HT22 cells lack functional ionotropic glutamate receptors and cause glutamate-mediated HT22 cell death [58]. Here, we demonstrated that kuwanon C treatment generates an effective antioxidant effect that protects against glutamate-induced ROS production, cellular damage, and cell death (Figure 6), confirming that this compound may have some value in the treatment of neurodegenerative diseases.

The initiating pathoetiology of neurodegenerative disorders involves an inflammatory process in response to a diverse array of CNS stimuli [59], and microglia, which are involved in the neuroinflammation process, are directly related to cognitive impairment and the neurodegenerative process [60]. Inflammation is a vital component of the immune response that protects against damage and infection. However, excessive acute or chronic inflammation can result in serious pathologies, including arthritis, asthma, inflammatory bowel disease, neurodegenerative disorders, and sepsis [61]. Macrophages play a prominent role in inflammatory diseases and produce a variety of inflammatory cytokines, including TNF- $\alpha$ , IL-1 $\beta$ , IL-6, and other inflammatory mediators induced by LPS. Macrophages also produce proinflammatory and cytotoxic mediators, including NO and prostaglandins (PGs), through the activity of their inducible enzymes, such as iNOS and COX-2 [61,62]. In macrophages, the NF- $\kappa$ B pathway is a master regulator of the molecular inflammatory response and is involved in the expression and production of proinflammatory mediators and cytokines. Under normal conditions, NF- $\kappa$ B is made up of inactive p50 and p65 subunits bound to the inhibitor of NF- $\kappa$ B (I $\kappa$ B- $\alpha$ ), but, when this pathway is activated by LPS or other stimuli, it phosphorylates I $\kappa$ B- $\alpha$ , leading to its degradation and the subsequent translocation of NF- $\kappa$ B into the nucleus [63]. Macrophage-like RAW264.7 and microglia-like BV2 cells are useful for evaluating these anti-inflammatory effects. In this study, we showed that kuwanon C effectively inhibited NO, PGE<sub>2</sub>, IL-6, and TNF- $\alpha$  production in BV2 and RAW264.7 cells (Figure 7). In addition, iNOS and COX-2 were also effectively inhibited by this compound (Figure 8), and NF- $\kappa$ B activation and its translocation into the nucleus were also inhibited by kuwanon C treatment (Figure 9). Because HO-1 and Nrf2 are known to be critical to the regulation of oxidative damage and inflammation in most cell types [4], we examined whether antioxidative and anti-inflammatory effects were directly related to the modification of their expression by testing the effects of kuwanon C in the presence of an HO-1 inhibitor. Using this approach, we confirmed that the antioxidative and anti-inflammatory effects of kuwanon C were mediated by HO-1 and Nrf2 in HT22, BV2, and RAW264.7 cells (Figure 10). These results suggest that HO-1 mediates the effects of kuwanon C and that these effects are regulated by the Nrf2 pathway.

The focus of this study is to find new activity of sixteen compounds isolated from *C. tricuspidata* through the HO-1 regulatory action in three different cell lines including HT22, BV2, and RAW264.7. We find that kuwanon C is shown to be an effective HO-1 inducer in three cell lines, which is critical for understanding inflammatory and oxidative stress responses. Therefore, this study has been meaningful as the first report that among the sixteen compounds kuwanon C was also shown to exert neuroprotective effects in HT22 cells, anti-inflammatory effects in RAW264.7, and anti-neuroinflammatory effects in BV2 cells via Nrf2-mediated HO-1 regulation. These results suggest that the mechanism of HO-1 regulation could be important in identifying neuroprotective or anti-inflammatory compounds derived from natural products, and may provide insights into future intervention strategies to treat neurodegenerative or inflammatory diseases. Based on the present study, the further studies are needed to use *C. tricuspidata* extract or kuwanon C for the commercial or wide uses. Finally, we think that *C. tricuspidata* extract or kuwanon C might be an advantageous candidate for the treatment of neurodegenerative or inflammatory diseases.

## 4. Materials and Methods

### 4.1. Materials

Tissue culture reagents, such as Roswell Park Memorial Institute 1640 (RPMI 1640), Dulbecco's Modified Eagle's Medium (DMEM), and fetal bovine serum (FBS), were purchased from Gibco BRL Co. (Grand Island, NY, USA). All chemicals were obtained from Sigma-Aldrich Chemical Co. (St. Louis, MO, USA). Primary antibodies, including anti-HO-1, anti-Nrf2, anti-p65, anti-COX-2, anti-iNOS, anti- $\beta$ -actin, and anti-proliferating cell nuclear antigen (PCNA) were purchased from Santa Cruz Biotechnology (Santa Cruz, CA, USA), and anti-rabbit and anti-mouse secondary antibodies were purchased from Millipore (Billerica, MA, USA). ELISA kits for PGE<sub>2</sub>, IL-6, and TNF- $\alpha$  were purchased

from R&D Systems, Inc. (Minneapolis, MN, USA). The structure of each of the sixteen *C. tricuspidata* compounds was determined by analyzing various spectroscopic data, including mass spectroscopy and nuclear magnetic resonance (NMR) data, which were consistent with what had been previously reported [10].

#### 4.2. Cell Culture and Viability Assays

HT22 and BV2 cells were donated by Prof. Youn-Chul Kim (College of Pharmacy, Wonkwang University, Iksan, Republic of Korea). RAW264.7 was purchased from American Type Culture Collection (ATCC, Manassas, VA, USA). HT22 cells were cultured in DMEM supplemented with 1% penicillin–streptomycin and 10% heat-inactivated FBS at 37 °C in a humidified 5% CO<sub>2</sub> and 95% air atmosphere. RAW264.7 and BV2 cells were maintained at  $5 \times 10^5$  cells/mL in RPMI 1640 supplemented with 10% heat-inactivated fetal bovine serum, L-glutamine (2 mM), penicillin G (100 units/mL), and streptomycin (100 mg/mL). The cell culture and viability assays were conducted according to a previously described method [20,64].

#### 4.3. Western Blot Analysis and Extraction of Cytoplasmic and Nuclear Cell Fractions

The pelleted HT22, RAW264.7, and BV2 cells were washed with phosphate-buffered saline (PBS) and subsequently lysed in radioimmunoprecipitation assay (RIPA) buffer. The cytoplasmic and nuclear fractions were extracted using the Caiman Nuclear Extraction Kit (Cayman, Ann Arbor, MI, USA), and each fraction was lysed according to the manufacturer's instructions. The detailed procedures for Western blot analysis were described in our previous report [64].

#### 4.4. Reactive Oxygen Species Generation Assays

To evaluate ROS generation, HT22 cells were incubated with glutamate (10 mM) with or without CTC 7 (10–40 μM) and SnPP (HO inhibitor) (50 μM). Treated cells were then incubated at 37 °C for 12 h after glutamate treatment, washed and treated with Hank's balanced salt solution containing 10 μM 2',7'-dichlorofluorescein diacetate (DCFDA), and placed in the dark for 60 min. Then, the medium was removed, the cells were washed twice, and extracted with 1% Triton X-100 in PBS at 37 °C for 10 min. The fluorescence of each sample was evaluated at 490 nm and 525 nm using a SpectraMax Gemini XS (Molecular Devices, Sunnyvale, CA, USA).

#### 4.5. Determination of Nitrite Concentrations

Nitrite, a stable end product of NO oxidation, was used as an indicator of NO production in each cell type, as previously described. [64,65].

#### 4.6. PGE<sub>2</sub> Assay

RAW264.7 and BV2 cells were cultured in 48-well plates, pretreated with different concentrations of CTC 7 for 3 h, and then stimulated with LPS (1 μg/mL) for 24 h. The culture media were collected to determine PGE<sub>2</sub> level present in each sample using a commercially available kit from R&D Systems, Inc. (Minneapolis, MN, USA). Three independent assays were performed according to the manufacturer's instruction.

#### 4.7. Assays for IL-6 and TNF-α

Culture medium was collected from each of the treatment groups and used to determine IL-6 and TNF-α expression using ELISA kits tailored to each collection process (R&D Systems, Inc., Minneapolis, MN, USA), according to the manufacturer's instructions. Briefly, RAW264.7 and BV2 cells were seeded in 48-well culture plates at a density of  $5 \times 10^5$  cells/well. After incubation, the supernatant was collected and used in the cytokine ELISA kits to measure the concentrations of IL-6 and TNF-α.

#### 4.8. NF- $\kappa$ B Localization and Immunofluorescence

To study the localization of NF- $\kappa$ B, RAW264.7 and BV2 cells were grown on Lab-Tek II chamber slides and treated with 40- $\mu$ M CTC 7 for 3 h before LPS stimulation (1  $\mu$ g/mL) for 1 h. Cells were then fixed in formalin and permeabilized using cold acetone. The detailed procedures were described in our previous report [66].

#### 4.9. Statistical Analysis

Data are presented as the mean  $\pm$  standard deviation for three or four independent experiments. One-way analysis of variance, followed by Tukey's multiple comparison tests, was used to compare the three groups. All statistical analyses were performed using GraphPad Prism software, version 5.01 (GraphPad Software Inc., San Diego, CA, USA).

### 5. Conclusions

Analysis of the bioactivity of sixteen compounds from the roots of *C. tricuspidata* revealed that the flavonoid compound kuwanon C exerts antioxidant effects in hippocampal cell lines and anti-inflammatory effects in both macrophage and microglial cell lines. In addition, this study demonstrates that the expression of HO-1 modulates cellular responses through the Nrf2 pathway. This study could provide the basis for clinical application of kuwanon C in the prevention and mitigation of oxidative injury.

**Supplementary Materials:** The following are available online at <http://www.mdpi.com/1422-0067/21/14/4839/s1>. Figure S1. Cytotoxicity of CTC 1-16 on HT22 cells. HT22 cells were treated with the various concentration of CTC 1-16 for 48 h. The viability of cells subjected to different concentrations of CTC 1-16 was determined by MTT assay. Data are presented as the mean standard deviation of three independent experiments. \*  $p < 0.05$ , \*\*  $p < 0.01$  vs. non-treated control. Figure S2. Cytotoxicity of CTC 1-16 on RAW264.7 cells. RAW264.7 cells were treated with the various concentration of CTC 1-16 for 48 h. The viability of cells subjected to different concentrations of CTC 1-16 was determined by MTT assay. Data are presented as the mean standard deviation of three independent experiments. \*  $p < 0.05$ , \*\*  $p < 0.01$ , \*\*\*  $p < 0.001$  vs. non-treated control. Figure S3. Cytotoxicity of CTC 1-16 on BV2 cells. BV2 cells were treated with the various concentration of CTC 1-16 for 48 h. The viability of cells subjected to different concentrations of CTC 1-16 was determined by MTT assay. Data are presented as the mean standard deviation of three independent experiments. \*\*  $p < 0.01$ , \*\*\*  $p < 0.001$  vs. non-treated control.

**Author Contributions:** Conceptualization, W.K., C.-S.Y., Y.-C.K., H.O., and D.-S.L.; Data curation, W.K., C.-S.Y., K.-W.K., H.L., N.K., and D.-S.L.; Formal analysis, C.-S.Y., Y.-C.K., H.O., and D.-S.L.; Funding acquisition, D.G.K., H.S.L., and D.-S.L.; Investigation, W.K., C.-S.Y., K.-W.K., H.L., N.K., and D.-S.L.; Resources, C.-S.Y., E.-R.W., Y.-C.K., and H.O.; Supervision, E.-R.W., Y.-C.K., D.G.K., H.S.L., H.O., and D.-S.L.; Visualization, W.K., C.-S.Y., K.-W.K., and D.-S.L.; Writing—original draft, W.K., C.-S.Y., K.-W.K., and D.-S.L.; Writing—review & editing, W.K., C.-S.Y., and D.-S.L. All authors have read and agreed to the published version of the manuscript.

**Funding:** This study was supported by the National Research Foundation of Korea (NRF) grants funded by the Korean government (NRF-2017R1A5A2015805 and NRF-2018R1C1B6001913).

**Conflicts of Interest:** The authors declare no conflict of interest.

### References

1. Yet, S.F.; Melo, L.G.; Layne, M.D.; Perrella, M.A. Heme Oxygenase 1 in Regulation of Inflammation and Oxidative Damage. In *Methods Enzymol*; Academic Press: Cambridge, MA, USA, 2002; Volume 353, pp. 163–176.
2. Elbirt, K.K.; Bonkovsky, H.L. Heme oxygenase: Recent advances in understanding its regulation and role. *Proc. Assoc. Am. Physicians* **1999**, *111*, 438–447. [[CrossRef](#)] [[PubMed](#)]
3. Ryter, S.W. Heme oxygenase-1/carbon monoxide as modulators of autophagy and inflammation. *Arch. Biochem. Biophys.* **2019**, *678*, 108186. [[CrossRef](#)] [[PubMed](#)]
4. Loboda, A.; Damulewicz, M.; Pyza, E.; Jozkowicz, A.; Dulak, J. Role of Nrf2/HO-1 system in development, oxidative stress response and diseases: An evolutionarily conserved mechanism. *Cell Mol. Life Sci.* **2016**, *73*, 3221–3247. [[CrossRef](#)]

5. Schipper, H.M. Heme oxygenase expression in human central nervous system disorders. *Free Radic. Biol. Med.* **2004**, *37*, 1995–2011. [[CrossRef](#)] [[PubMed](#)]
6. Xin, L.-T.; Yue, S.-J.; Fan, Y.-C.; Wu, J.-S.; Yan, D.; Guan, H.-S.; Wang, C.-Y. *Cudrania tricuspidata*: An updated review on ethnomedicine, phytochemistry and pharmacology. *RSC Adv.* **2017**, *7*, 31807–31832. [[CrossRef](#)]
7. Jeong, G.S.; An, R.B.; Pae, H.O.; Chung, H.T.; Yoon, K.H.; Kang, D.G.; Lee, H.S.; Kim, Y.C. Cudraticusxanthone A protects mouse hippocampal cells against glutamate-induced neurotoxicity via the induction of heme oxygenase-1. *Planta Med.* **2008**, *74*, 1368–1373. [[CrossRef](#)]
8. Jeong, G.S.; Lee, D.S.; Kim, Y.C. Cudraticusxanthone A from *Cudrania tricuspidata* suppresses pro-inflammatory mediators through expression of anti-inflammatory heme oxygenase-1 in RAW264.7 macrophages. *Int. Immunopharmacol.* **2009**, *9*, 241–246. [[CrossRef](#)]
9. Kim, K.W.; Quang, T.H.; Ko, W.; Kim, D.C.; Yoon, C.S.; Oh, H.; Kim, Y.C. Anti-neuroinflammatory effects of cudraflavanone A isolated from the chloroform fraction of *Cudrania tricuspidata* root bark. *Pharm. Biol.* **2018**, *56*, 192–200. [[CrossRef](#)]
10. Quang, T.H.; Ngan, N.T.; Yoon, C.S.; Cho, K.H.; Kang, D.G.; Lee, H.S.; Kim, Y.C.; Oh, H. Protein Tyrosine Phosphatase 1B Inhibitors from the Roots of *Cudrania tricuspidata*. *Molecules* **2015**, *20*, 11173–11183. [[CrossRef](#)]
11. Hatzieremia, S.; Gray, A.I.; Ferro, V.A.; Paul, A.; Plevin, R. The effects of cardamonin on lipopolysaccharide-induced inflammatory protein production and MAP kinase and NFkappaB signalling pathways in monocytes/macrophages. *Br. J. Pharmacol.* **2006**, *149*, 188–198. [[CrossRef](#)]
12. Drummond, G.S.; Baum, J.; Greenberg, M.; Lewis, D.; Abraham, N.G. HO-1 overexpression and underexpression: Clinical implications. *Arch. Biochem. Biophys.* **2019**, *673*, 108073. [[CrossRef](#)] [[PubMed](#)]
13. Bolisetty, S.; Zarjou, A.; Agarwal, A. Heme Oxygenase 1 as a Therapeutic Target in Acute Kidney Injury. *Am. J. Kidney Dis.* **2017**, *69*, 531–545. [[CrossRef](#)] [[PubMed](#)]
14. Rochette, L.; Zeller, M.; Cottin, Y.; Vergely, C. Redox Functions of Heme Oxygenase-1 and Biliverdin Reductase in Diabetes. *Trends Endocrinol. Metab.* **2018**, *29*, 74–85. [[CrossRef](#)] [[PubMed](#)]
15. Gagnière, J.; Bonnet, M. Molecular Mechanism Underlying the Actions of Antioxidant Molecules in Digestive Disorders. In *Gastrointestinal Tissue*; Academic Press: Cambridge, MA, USA, 2017; pp. 197–216.
16. Chen, J. Heme oxygenase in neuroprotection: From mechanisms to therapeutic implications. *Rev. Neurosci.* **2014**, *25*, 269–280. [[CrossRef](#)] [[PubMed](#)]
17. Ryter, S.W.; Choi, A.M. Targeting heme oxygenase-1 and carbon monoxide for therapeutic modulation of inflammation. *Transl Res.* **2016**, *167*, 7–34. [[CrossRef](#)]
18. Kim, D.C.; Lee, D.S.; Ko, W.; Kim, K.W.; Kim, H.J.; Yoon, C.S.; Oh, H.; Kim, Y.C. Heme Oxygenase-1-Inducing Activity of 4-Methoxydalbergione and 4'-Hydroxy-4-methoxydalbergione from *Dalbergia odorifera* and Their Anti-inflammatory and Cytoprotective Effects in Murine Hippocampal and BV2 Microglial Cell Line and Primary Rat Microglial Cells. *Neurotox. Res.* **2018**, *33*, 337–352.
19. Kim, K.W.; Yoon, C.S.; Kim, Y.C.; Oh, H. Desoxo-narchinol A and Narchinol B Isolated from *Nardostachys jatamansi* Exert Anti-neuroinflammatory Effects by Up-regulating of Nuclear Transcription Factor Erythroid-2-Related Factor 2/Heme Oxygenase-1 Signaling. *Neurotox. Res.* **2019**, *35*, 230–243. [[CrossRef](#)]
20. Lee, H.; Ko, W.; Chowdhury, A.; Li, B.; Kim, S.C.; Oh, H.; Kim, Y.C.; Woo, E.R.; Baek, N.I.; Lee, D.S. Brassicaphenanthrene A from *Brassica rapa* protects HT22 neuronal cells through the regulation of Nrf2-mediated heme oxygenase1 expression. *Mol. Med. Rep.* **2020**, *21*, 493–500.
21. Su, B.N.; Cuendet, M.; Hawthorne, M.E.; Kardono, L.B.; Riswan, S.; Fong, H.H.; Mehta, R.G.; Pezzuto, J.M.; Kinghorn, A.D. Constituents of the bark and twigs of *Artocarpus dadah* with cyclooxygenase inhibitory activity. *J. Nat. Prod.* **2002**, *65*, 163–169. [[CrossRef](#)]
22. Zheng, Z.P.; Cheng, K.W.; To, J.T.; Li, H.; Wang, M. Isolation of tyrosinase inhibitors from *Artocarpus heterophyllus* and use of its extract as antibrowning agent. *Mol. Nutr. Food Res.* **2008**, *52*, 1530–1538. [[CrossRef](#)]
23. Zheng, Z.P.; Tan, H.Y.; Chen, J.; Wang, M. Characterization of tyrosinase inhibitors in the twigs of *Cudrania tricuspidata* and their structure-activity relationship study. *Fitoterapia* **2013**, *84*, 242–247. [[CrossRef](#)]
24. Jin, Y.J.; Lin, C.C.; Lu, T.M.; Li, J.H.; Chen, I.S.; Kuo, Y.H.; Ko, H.H. Chemical constituents derived from *Artocarpus xanthocarpus* as inhibitors of melanin biosynthesis. *Phytochemistry* **2015**, *117*, 424–435. [[CrossRef](#)]
25. Nguyen, H.X.; Nguyen, N.T.; Nguyen, M.H.; Le, T.H.; Van Do, T.N.; Hung, T.M.; Nguyen, M.T. Tyrosinase inhibitory activity of flavonoids from *Artocarpus heterophyllous*. *Chem. Cent. J.* **2016**, *10*, 2. [[CrossRef](#)]

26. Zhang, L.; Tao, G.; Chen, J.; Zheng, Z.P. Characterization of a New Flavone and Tyrosinase Inhibition Constituents from the Twigs of *Morus alba* L. *Molecules* **2016**, *21*, 1130. [[CrossRef](#)]
27. Kim, D.C.; Quang, T.H.; Oh, H.; Kim, Y.C. Steppogenin Isolated from *Cudrania tricuspidata* Shows Antineuroinflammatory Effects via NF-kappaB and MAPK Pathways in LPS-Stimulated BV2 and Primary Rat Microglial Cells. *Molecules* **2017**, *22*, 2130. [[CrossRef](#)] [[PubMed](#)]
28. Rho, Y.H.; Lee, B.W.; Park, K.H.; Bae, Y.S. Cudraflavanone A purified from *Cudrania tricuspidata* induces apoptotic cell death of human leukemia U937 cells, at least in part, through the inhibition of DNA topoisomerase I and protein kinase C activity. *Anticancer Drugs* **2007**, *18*, 1023–1028. [[CrossRef](#)] [[PubMed](#)]
29. Han, H.J.; Kim, T.J.; Jin, Y.R.; Hong, S.S.; Hwang, J.H.; Hwang, B.Y.; Lee, K.H.; Park, T.K.; Yun, Y.P. Cudraflavanone A, a flavonoid isolated from the root bark of *Cudrania tricuspidata*, inhibits vascular smooth muscle cell growth via an Akt-dependent pathway. *Planta Med.* **2007**, *73*, 1163–1168. [[CrossRef](#)] [[PubMed](#)]
30. Groweiss, A.; Cardellina, J.H.; Boyd, M.R. HIV-Inhibitory prenylated xanthenes and flavones from *Maclura tinctoria*. *J. Nat. Prod.* **2000**, *63*, 1537–1539. [[CrossRef](#)]
31. Tian, Y.H.; Kim, H.C.; Cui, J.M.; Kim, Y.C. Hepatoprotective constituents of *Cudrania tricuspidata*. *Arch. Pharm Res.* **2005**, *28*, 44–48. [[CrossRef](#)]
32. Lee, B.W.; Gal, S.W.; Park, K.M.; Park, K.H. Cytotoxic xanthenes from *Cudrania tricuspidata*. *J. Nat. Prod.* **2005**, *68*, 456–458. [[CrossRef](#)]
33. Zou, Y.S.; Hou, A.J.; Zhu, G.F. Isoprenylated xanthenes and flavonoids from *Cudrania tricuspidata*. *Chem Biodivers* **2005**, *2*, 131–138. [[CrossRef](#)] [[PubMed](#)]
34. Ko, H.H.; Yu, S.M.; Ko, F.N.; Teng, C.M.; Lin, C.N. Bioactive constituents of *Morus australis* and *Broussonetia papyrifera*. *J. Nat. Prod.* **1997**, *60*, 1008–1011. [[CrossRef](#)] [[PubMed](#)]
35. Chi, Y.S.; Jong, H.G.; Son, K.H.; Chang, H.W.; Kang, S.S.; Kim, H.P. Effects of naturally occurring prenylated flavonoids on enzymes metabolizing arachidonic acid: Cyclooxygenases and lipoxygenases. *Biochem. Pharmacol.* **2001**, *62*, 1185–1191. [[CrossRef](#)]
36. Lee, N.K.; Son, K.H.; Chang, H.W.; Kang, S.S.; Park, H.; Heo, M.Y.; Kim, H.P. Prenylated flavonoids as tyrosinase inhibitors. *Arch. Pharm. Res.* **2004**, *27*, 1132–1135. [[CrossRef](#)]
37. Chaita, E.; Lambrinidis, G.; Cheimonidi, C.; Agalou, A.; Beis, D.; Trougakos, I.; Mikros, E.; Skaltsounis, A.L.; Aligiannis, N. Anti-Melanogenic Properties of Greek Plants. A Novel Depigmenting Agent from *Morus alba* Wood. *Molecules* **2017**, *22*, 514. [[CrossRef](#)]
38. Sohn, H.Y.; Son, K.H.; Kwon, C.S.; Kwon, G.S.; Kang, S.S. Antimicrobial and cytotoxic activity of 18 prenylated flavonoids isolated from medicinal plants: *Morus alba* L., *Morus mongolica* Schneider, *Broussonetia papyrifera* (L.) Vent, *Sophora flavescens* Ait and *Echinosophora koreensis* Nakai. *Phytomedicine* **2004**, *11*, 666–672. [[CrossRef](#)]
39. Arung, E.T.; Shimizu, K.; Kondo, R. Inhibitory effect of isoprenoid-substituted flavonoids isolated from *Artocarpus heterophyllus* on melanin biosynthesis. *Planta Med.* **2006**, *72*, 847–850. [[CrossRef](#)]
40. Ferlinahayati; Syah, Y.M.; Juliawaty, L.D.; Achmad, S.A.; Hakim, E.H.; Takayama, H.; Said, I.M.; Latip, J. Phenolic constituents from the wood of *Morus australis* with cytotoxic activity. *Z. Naturforsch. C J. Biosci.* **2008**, *63*, 35–39. [[CrossRef](#)]
41. Arung, E.T.; Yoshikawa, K.; Shimizu, K.; Kondo, R. Isoprenoid-substituted flavonoids from wood of *Artocarpus heterophyllus* on B16 melanoma cells: Cytotoxicity and structural criteria. *Fitoterapia* **2010**, *81*, 120–123. [[CrossRef](#)] [[PubMed](#)]
42. Kim, J.Y.; Lee, W.S.; Kim, Y.S.; Curtis-Long, M.J.; Lee, B.W.; Ryu, Y.B.; Park, K.H. Isolation of cholinesterase-inhibiting flavonoids from *Morus lhou*. *J. Agric. Food Chem.* **2011**, *59*, 4589–4596. [[CrossRef](#)] [[PubMed](#)]
43. Arung, E.T.; Shimizu, K.; Kondo, R. *Artocarpus* plants as a potential source of skin whitening agents. *Nat. Prod. Commun.* **2011**, *6*, 1397–1402. [[CrossRef](#)] [[PubMed](#)]
44. Yang, Z.G.; Matsuzaki, K.; Takamatsu, S.; Kitanaka, S. Inhibitory effects of constituents from *Morus alba* var. *multicaulis* on differentiation of 3T3-L1 cells and nitric oxide production in RAW264.7 cells. *Molecules* **2011**, *16*, 6010–6022. [[CrossRef](#)] [[PubMed](#)]
45. Zelova, H.; Hanakova, Z.; Cermakova, Z.; Smejkal, K.; Dall Acqua, S.; Babula, P.; Cvacka, J.; Hosek, J. Evaluation of anti-inflammatory activity of prenylated substances isolated from *Morus alba* and *Morus nigra*. *J. Nat. Prod.* **2014**, *77*, 1297–1303. [[CrossRef](#)]

46. Cheon, B.S.; Kim, Y.H.; Son, K.S.; Chang, H.W.; Kang, S.S.; Kim, H.P. Effects of prenylated flavonoids and biflavonoids on lipopolysaccharide-induced nitric oxide production from the mouse macrophage cell line RAW 264.7. *Planta Med.* **2000**, *66*, 596–600. [[CrossRef](#)] [[PubMed](#)]
47. Abbas, G.M.; Abdel Bar, F.M.; Baraka, H.N.; Gohar, A.A.; Lahloub, M.F. A new antioxidant stilbene and other constituents from the stem bark of *Morus nigra* L. *Nat. Prod. Res.* **2014**, *28*, 952–959. [[CrossRef](#)] [[PubMed](#)]
48. Lin, Q.H.; Yuan, J.B.; Ma, Z.L.; Liang, J.; Zhai, X.X.; Khan, I.A.; Ding, Y.Q.; Ren, G. Isoprenylated Flavonoids from Roots of *Artocarpus styracfolius*. *Nat. Prod. Commun.* **2016**, *11*, 1843–1846. [[PubMed](#)]
49. Hou, X.D.; Ge, G.B.; Weng, Z.M.; Dai, Z.R.; Leng, Y.H.; Ding, L.L.; Jin, L.L.; Yu, Y.; Cao, Y.F.; Hou, J. Natural constituents from Cortex *Mori Radicis* as new pancreatic lipase inhibitors. *Bioorg. Chem.* **2018**, *80*, 577–584. [[CrossRef](#)]
50. Xia, P.; Gao, X.; Duan, L.; Zhang, W.; Sun, Y.F. Mulberrin (Mul) reduces spinal cord injury (SCI)-induced apoptosis, inflammation and oxidative stress in rats via miRNA-337 by targeting Nrf-2. *Biomed. Pharmacother.* **2018**, *107*, 1480–1487. [[CrossRef](#)]
51. Abdel Bar, F.M.; Abbas, G.M.; Gohar, A.A.; Lahloub, M.I. Antiproliferative activity of stilbene derivatives and other constituents from the stem bark of *Morus nigra* L. *Nat. Prod. Res.* **2019**, 1–8. [[CrossRef](#)]
52. Cao, W.; Dong, Y.; Zhao, W.; Lu, X.; Sun, L. Mulberrin attenuates 1-methyl-4-phenyl-1,2,3,6-tetrahydropyridine (MPTP)-induced Parkinson's disease by promoting Wnt/beta-catenin signaling pathway. *J. Chem. Neuroanat.* **2019**, *98*, 63–70. [[CrossRef](#)] [[PubMed](#)]
53. Lee, J.M.; Calkins, M.J.; Chan, K.; Kan, Y.W.; Johnson, J.A. Identification of the NF-E2-related factor-2-dependent genes conferring protection against oxidative stress in primary cortical astrocytes using oligonucleotide microarray analysis. *J. Biol. Chem.* **2003**, *278*, 12029–12038. [[CrossRef](#)]
54. Lee, D.S.; Jeong, G.S. Butein provides neuroprotective and anti-neuroinflammatory effects through Nrf2/ARE-dependent haem oxygenase 1 expression by activating the PI3K/Akt pathway. *Br. J. Pharmacol.* **2016**, *173*, 2894–2909. [[CrossRef](#)] [[PubMed](#)]
55. Keller, J.N.; Mattson, M.P. Roles of lipid peroxidation in modulation of cellular signaling pathways, cell dysfunction, and death in the nervous system. *Rev. Neurosci.* **1998**, *9*, 105–116. [[CrossRef](#)]
56. Simonian, N.A.; Coyle, J.T. Oxidative stress in neurodegenerative diseases. *Annu. Rev. Pharmacol. Toxicol.* **1996**, *36*, 83–106. [[CrossRef](#)] [[PubMed](#)]
57. Rossler, O.G.; Bauer, I.; Chung, H.Y.; Thiel, G. Glutamate-induced cell death of immortalized murine hippocampal neurons: Neuroprotective activity of heme oxygenase-1, heat shock protein 70, and sodium selenite. *Neurosci. Lett.* **2004**, *362*, 253–257. [[CrossRef](#)]
58. Lee, D.S.; Cheong, S.H. Taurine Have Neuroprotective Activity against Oxidative Damage-Induced HT22 Cell Death through Heme Oxygenase-1 Pathway. *Adv. Exp. Med. Biol.* **2017**, *975 Pt 1*, 159–171.
59. Suescun, J.; Chandra, S.; Schiess, M.C. The Role of Neuroinflammation in Neurodegenerative Disorders. In *Translational Inflammation*; Academic Press: Cambridge, MA, USA, 2019; pp. 241–267.
60. Yuste, J.E.; Tarragon, E.; Campuzano, C.M.; Ros-Bernal, F. Implications of glial nitric oxide in neurodegenerative diseases. *Front. Cell Neurosci.* **2015**, *9*, 322. [[CrossRef](#)] [[PubMed](#)]
61. Lucas, K.; Maes, M. Role of the Toll Like receptor (TLR) radical cycle in chronic inflammation: Possible treatments targeting the TLR4 pathway. *Mol. Neurobiol.* **2013**, *48*, 190–204. [[CrossRef](#)] [[PubMed](#)]
62. Karpurapu, M.; Wang, X.; Deng, J.; Park, H.; Xiao, L.; Sadikot, R.T.; Frey, R.S.; Maus, U.A.; Park, G.Y.; Scott, E.W.; et al. Functional PU.1 in macrophages has a pivotal role in NF-kappaB activation and neutrophilic lung inflammation during endotoxemia. *Blood* **2011**, *118*, 5255–5266. [[CrossRef](#)]
63. Dorrington, M.G.; Fraser, I.D.C. NF-kappaB Signaling in Macrophages: Dynamics, Crosstalk, and Signal Integration. *Front. Immunol.* **2019**, *10*, 705. [[CrossRef](#)]
64. Ko, W.; Sohn, J.H.; Jang, J.H.; Ahn, J.S.; Kang, D.G.; Lee, H.S.; Kim, J.S.; Kim, Y.C.; Oh, H. Inhibitory effects of alternaramide on inflammatory mediator expression through TLR4-MyD88-mediated inhibition of NF-κB and MAPK pathway signaling in lipopolysaccharide-stimulated RAW264.7 and BV2 cells. *Chem. Biol. Interact.* **2016**, *244*, 16–26. [[CrossRef](#)] [[PubMed](#)]

65. Titheradge, M.A. The enzymatic measurement of nitrate and nitrite. *Methods Mol. Biol.* **1998**, *100*, 83–91. [[PubMed](#)]
66. Kim, D.C.; Yoon, C.S.; Quang, T.H.; Ko, W.; Kim, J.S.; Oh, H.; Kim, Y.C. Prenylated Flavonoids from *Cudrania tricuspidata* Suppress Lipopolysaccharide-Induced Neuroinflammatory Activities in BV2 Microglial Cells. *Int. J. Mol. Sci.* **2016**, *17*, 255. [[CrossRef](#)] [[PubMed](#)]



© 2020 by the authors. Licensee MDPI, Basel, Switzerland. This article is an open access article distributed under the terms and conditions of the Creative Commons Attribution (CC BY) license (<http://creativecommons.org/licenses/by/4.0/>).